From Basic Network Principles to Neural Architecture: Emergence of Orientation-Selective Cells

Ralph Linsker

PNAS 1986;83;8390-8394
doi:10.1073/pnas.83.21.8390

Proc. Natl. Acad. Sci. USA
Vol. 83, pp. 8390–8394, November 1986
Neurobiology

From basic network principles to neural architecture: Emergence of orientation-selective cells*

(modular self-adaptive networks/visual system/feature-analyzing cells)

RALPH LINSKER

IBM Thomas J. Watson Research Center, Yorktown Heights, NY 10598

Communicated by Richard L. Garwin, July 7, 1986

ABSTRACT **This is the second paper in a series of three that explores the emergence of several prominent features of the functional architecture of visual cortex, in a "modular self-adaptive network" containing several layers of cells with parallel feedforward connections whose strengths develop according to a Hebb-type correlation-rewarding rule. In the present paper I show that orientation-selective cells, similar to the "simple" cortical cells of Hubel and Wiesel [Hubel, D. H. & Wiesel, T. N. (1962) *J. Physiol.* 160, 106–154], emerge in such a network. No orientation preference is specified to the system at any stage, the orientation-selective cell layer emerges even in the absence of environmental input to the system, and none of the basic developmental rules is specific to visual processing.**

In this series of papers, I show that many observed features of the functional architecture of mammalian visual cortex emerge in a simple system consisting of several layers of cells developing under the influence of a connection-modification rule (e.g., of Hebb type). Paper 1 (1) showed the emergence of spatial-opponent cells in a three-layer system with parallel feedforward connections only and with random spontaneous activity (no environmental input needed) in the first layer.

In the present paper, I extend the network of paper 1 by adding more layers to the system and retaining the same development rule used in paper 1. I show that when a set of uncorrelated activities is randomly generated in the first layer (layer A) of the system and processed by the mature A-to-B and (opponent-type) B-to-C connections whose emergent properties were derived in paper 1, the layer-C activity displays spatial structure. That is, the activities of a pair of cells in layer C are correlated over distances of the order of the arborization breadth of the B-to-C connections. Further, the particular ("Mexican-hat") form of this two-point autocorrelation function leads to the emergence of orientation-selective cells in later layers of the system. These cells' receptive field properties are similar to those of the "simple" cells of Hubel and Wiesel (2).

Orientation-Selective Cells. Orientation-selective cells organized into "columns"—bandlike regions of cells of the same or similar orientation—are found in all layers except IVa and IVc of area 17 in macaque monkey (3, 4), and have also been described in cat and other mammalian systems. In macaque, these cells and organization arise prior to any visual experience (4).

Several suggestions have been made concerning the origin and organization of orientation-selective cells. (*i*) Anisotropies in retinal anatomy (e.g., in cat) might somehow induce horizontal and vertical orientation preferences in specific groups of fibers (5), or groups of orientation-specific fibers can be postulated *ab initio* (6), and a lateral-inhibition mechanism can be invoked to "fill in" the intermediate orientations. (*ii*) Input from other systems (e.g., vestibular) could somehow play a role in the formation of orientation-selective cells. (*iii*) For a model environment consisting of bar patterns at all orientations, centered one at a time over a cell whose inputs are arranged to form a ring, and with an assumed mechanism that forces the cell to discriminate among patterns, it has been found that the response of the cell becomes tuned to a particular orientation preference (7). (*iv*) Certain cells may serve as organizing centers that induce the formation of orientation-selective cells with a particular disposition of preferred orientations, accounting for the observed columnar arrangement (8).

These previous studies have contributed to a framework for thinking about the conditions under which orientation-selective cells might form. They have not, however, produced an explicit theory of how (or whether) orientation-selective cells can form—either in a realistic visual environment or in the absence of visual input—without somehow specifying at least some orientation preferences to the system at the outset.

The present paper is concerned with the following questions. Can a layer of orientation-selective cells emerge in the absence of visual experience, with no built-in anisotropies or orientation preferences and with no input from other systems that may be interacting with the external environment? In particular, does such a cell layer emerge in a modular (layered) self-adaptive network (1) governed by some simple, biologically plausible rules for synaptic modification and for the basic structure of a network, and given only spontaneous electrical activity (no environmental interaction)? If it does, does its formation depend upon precisely chosen conditions, or upon qualitative features that are rather general?

METHODS

Gross Architecture and Development Rule. The gross architecture of our system is that of paper 1, extended to additional layers D, E, . . ., in the identical manner as in figure 1 of paper 1. The ensemble-averaged development rule for the connection strength c_{ni} of the ith synaptic input to any given postsynaptic cell (indexed by n) of layer M (M = D, E, . . .) is the same as that derived in paper 1:

$$\dot{c}_{ni} = k_1 + k_2 g_n + \frac{1}{N_M} \sum_j Q^L_{\mathrm{pre}(ni),\mathrm{pre}(nj)} c_{nj}, \qquad [1]$$

where $g_n \equiv (\Sigma_j c_{nj})/N_M$, there are N_M synaptic inputs to each M cell, and k_1 and k_2 are parameter values (the same for all cells of layer M). Here L denotes the layer that supplies input to the cells of layer M, "pre(ni)" denotes the L cell that is presynaptic to the ith synapse of cell n, and $Q^L_{ab} \propto \langle (F^{L\pi}_a - \bar{F}^L) \times (F^{L\pi}_b - \bar{F}^L) \rangle_\pi$, which for our system is proportional to the two-point autocorrelation function of the activities at L

The publication costs of this article were defrayed in part by page charge payment. This article must therefore be hereby marked "*advertisement*" in accordance with 18 U.S.C. §1734 solely to indicate this fact.

*This is paper no. 2 in a series. Paper no. 1 is ref. 1.

cells a and b, averaged over an ensemble of activity "presentations" indexed by π (see paper 1 for details). Since we shall be referring to the properties of more than one M cell at a time, I have added the M-cell index n to our notation and have subscripted Q^{L} (and the activity $F^{L\pi}$) according to the L cells whose activities they describe, rather than by the indices of the synaptic inputs to a particular M cell (as was simplest in paper 1).

Once the L-to-M connections have matured, the corresponding Q function for layer M is given by

$$Q^{M}_{nm} \propto \sum_i \sum_j Q^{L}_{\mathrm{pre}(ni),\mathrm{pre}(mj)} c_{ni} c_{mj}, \qquad [2]$$

where n and m are the indices of two cells in layer M, i ranges over the synaptic inputs to cell n, and j ranges over the inputs to cell m. To derive this, use (from paper 1) $Q^{M}_{nm} \propto \langle (F^{M\pi}_{n} - \bar{F}^{M}) \times (F^{M\pi}_{m} - \bar{F}^{M}) \rangle_{\pi} \propto \langle [\sum_i c_{ni} (F^{L\pi}_{\mathrm{pre}(ni)} - \bar{F}^{L})] \times [\sum_j c_{mj} (F^{L\pi}_{\mathrm{pre}(mj)} - \bar{F}^{L})] \rangle_{\pi}$, bring the summations and c factors outside the ensemble-averaging brackets $\langle \ldots \rangle_{\pi}$, and use the definition of $Q^{L}_{\mathrm{pre}(ni),\mathrm{pre}(mj)}$.

Calculations. To calculate the development of a set of M cells, we carry out the program described in paper 1. Some practical notes: (*i*) When surveying the parameter space, we generally use $N_M = 300$ synapses, placed either randomly or on a polar grid [at sites (r, ϕ) spaced uniformly in angle ϕ and in $z \equiv \exp(-r^2/r_M^2)$, to give the correct Gaussian synaptic density (1)]. Placement on such a regular grid allows us to eliminate the random density fluctuations that are otherwise much more prominent for small N_M (of 300) than for the larger N_M (up to many thousands) that are of biological interest. More detailed runs are then done using N_M of 600, with random (as well as polar-grid) placements. (*ii*) For most runs, all c values are bounded by $n_{EM} - 1$ and n_{EM} (n_{EM} is one of the four parameters that define the morphologic regime, along with k_1, k_2, and r_M/r_L). Some runs are repeated using two classes of synapses (excitatory and inhibitory) with c value limits of 0,1 and -1,0 respectively; the same mature cell morphologies emerge (1). (*iii*) The particular distribution from which initial c values are randomly drawn is found generally not to affect the mature morphology. We usually use a uniform distribution on the interval -0.5 to 0.5 (if these are the c limits), but the same results are obtained by using a highly biased distribution, such as one uniform on -0.5 to -0.3, or by using a normal distribution.

The Concept of "Hebb-Optimal" States. At this point I introduce a powerful tool for understanding the character of the mature states in this type of system. Let us define an "energy" or "objective function" corresponding to Eq. 1, for a single M cell labeled n (recall that $g_n \equiv (\sum_j c_{nj})/N_M$):

$$E_n(c_{n1}, c_{n2}, \ldots) \equiv -k_1 g_n - \frac{k_2}{2} g_n^2 - \frac{1}{2N_M^2} \sum_i \sum_j Q^{L}_{\mathrm{pre}(ni),\mathrm{pre}(nj)} c_{ni} c_{nj}. \qquad [3]$$

Since $\dot{c}_{ni} = -N_M (\partial E_n/\partial c_{ni})$ for each i, we see that the development Eq. 1 changes the c values in such a way that the corresponding point in configuration space—which has N_M coordinates, the value of the ith coordinate being c_{ni}—moves along the path of locally steepest descent of E_n (i.e., the path of gradient descent) at each time step.

Starting from a random set of c values one is therefore guaranteed to arrive, for each cell n, at a local (though not necessarily a global) minimum of E_n, with each c [or each c but one per M cell (1)] saturating at one of its two limiting values. As an empirical matter, however, I find that in practically all cases studied the E_n values of mature configurations obtained using Eq. 1 (for various random initial conditions) overlap the globally near-minimal values of E_n obtained by using the method of "simulated annealing" (9). That is, Eq. 1 finds *global* near-minima of E_n for each cell n of layer M. Also, at transitions from one morphologic regime to another, where two morphologies can emerge for the same set of parameters but different choices of initial c values and/or random synaptic positions, the two solutions have similar, and globally near-minimal, energy. I emphasize that this global near-minimizing action of Eq. 1 is an empirical finding; its limits of validity have not been established.

The only exception that has been found occurs when k_2 is positive and a "ridge" of high E_n value, lying at $g \simeq -k_1/k_2$, separates the configuration space into two parts [e.g., see layer-B development regime (*iii*) in paper 1]. Then the configuration moves "downhill" from whatever its initial g value is to reach the maximum or minimum possible g value—i.e., to become "all-excitatory" or "all-inhibitory." This is also the only exception I have found to the irrelevance of initial c values to mature morphology.

It is therefore very useful to study the states having energy at or near the global energy minimum. We will call such states "nearly Hebb-optimal" since the E_n function of Eq. 3 is the unique objective function (apart from an irrelevant constant) for the development Eq. 1, which is based on Hebb-type modification.

RESULTS

The System Through Layer C. We build upon the results of paper 1. Layer B consists of "all-excitatory" cells. Q^{B}_{nm} is, apart from random cell-to-cell variations which become small in the limit that the number of synapses per cell is large (1), a function, denoted $Q^{B}(s)$, only of the distance s between cells n and m: $Q^{B}(s) = \exp(-a^{B}s^2/2)$.

We choose layer-C development parameter values to lie in the "ON-center" opponent-cell regime. An illustrative choice of values is $n_{EC} = 0.5$, $r_C/r_B = (5)^{1/2}$, $k_1 = 0.35$, $k_2 = -3$. For $N_C = 600$ with random synaptic placement, this set of values yields ON-center C cells that are substantially circularly symmetric (the center of the excitatory core is typically displaced 0.1–0.2 r_C from the cell's center) with $g = 0.126 \pm 0.001$.

"Mexican-Hat" Activity Autocorrelation Function. When Q^{M}_{nm} is computed for any pair of these explicitly generated C cells at a variety of relative positions, it has a Mexican-hat form: positive (correlated activities) when the cells' cores overlie one another; negative (anticorrelated activities) at intermediate displacements for which each core overlies the inhibitory surround of the other cell; and zero when the cells are remote from each other.

The analysis of a layer of cells each having a randomly displaced core is computationally much more demanding than that for a layer of cells that can each be taken to be circularly symmetric. Furthermore, the simpler analysis is far more instructive: it allows us to lay bare the essential feature that results in the emergence of orientation selectivity in later layers.

To proceed with the calculation, we therefore adopt an idealization in which Q^{C}_{nm} (as a function of the separation s between n and m) depends only upon s and is independent of which particular cells n and m are chosen. That is, a single Mexican-hat function of s, denoted $Q^{C}(s)$, will be used to compute all Q^{C}_{nm} values. This corresponds to adopting an idealized version of layer C, in which each cell is circularly symmetric with core radius of $r_{core}/r_C = 0.99$ [the value appropriate to this $g = 0.126$ and $n_{EC} = 0.5$ (1)]. Calculation of the effect of deviations from this idealization on the development of later layers is beyond the scope of this paper.

There are two aspects to this idealization, and to its validity. First, random cell-to-cell morphologic variations result from the random placement of the N_M synaptic inputs

to each cell; these variations are small in the limit that N_M is large. Second, the mature morphology shows a consistent deviation from circular symmetry when the mature g value is small (1), even when a symmetric (polar-grid) placement of synapses is used in the simulation. (The direction of core shift for any particular cell is random and is determined in the symmetric-placement case by the random choice of initial c values.) This asymmetry is reduced by increasing $\bar{k} \equiv -k_1/k_2$, thereby increasing the value of g at maturity. A detailed analysis of the conditions under which the results (for later layers) of the idealized calculation break down would set limits on how small g should be chosen to be. In this paper I wish rather to emphasize the essential features that emerge as a result of Mexican-hat-type activity correlation in layer C without dwelling on the choice of "best" mature g value.

The emergence of orientation-selective cells does not depend sensitively upon the g value in any particular layer. A larger g gives a Mexican-hat Q function with a shallower minimum, but allowing a series of opponent-cell layers to develop in series (as we shall do) deepens this minimum. Any developing layer "sees" only the Q function at its predecessor layer. Whether that function results from having a few opponent layers with small g values or more layers with larger g values is irrelevant to cell development.

From Layer C to D. To derive $Q^C(s)$ for a C layer of circularly symmetric cells, note that Eq. 2 (with L = B, M = C) becomes, in the large-N_C (continuum) limit, $Q^C(s) \propto \int d^2u \int d^2u'\, Q^B(|s + u' - u|)\, c(u)\, c(u')$, where $c(u) = n_{EC}$ for $|u| < r_{core}$ and $(n_{EC} - 1)$ for $|u| > r_{core}$. Here u and u' correspond to the positions of synapses ni and mj (Eq. 2) relative to their cells' centers, and s is the position of cell m relative to cell n.

For the case $n_{EC} = 0.5$, $r_C/r_B = (5)^{1/2}$, $r_{core}/r_C = 0.99$ (see above), $Q^C(s)$ is maximal at $s = 0$ (where we normalize it to equal 1), passes through 0 at $s = 1.27r_C$, reaches its minimum of -0.13 at $s_{min} = 1.74r_C$, and has absolute value <0.01 for $s > 2.7r_C$. For comparison, a minimum of -0.21 would be achieved if we could have a layer of circularly symmetric opponent cells with $g = 0$, which is not realizable in layer C of our system. (This does not rule out the possibility of obtaining such opponent cells in a system with different gross architecture.)

This Q^C function now leads to a spectrum of morphologic options for layer D, depending upon the parameter values for layer-D development. Rather than discuss these options here, I shall show how our network can generate Q functions having progressively more pronounced Mexican-hat character—i.e., with a deeper minimum relative to the peak at $s = 0$. Briefly, the morphologic options for layer D are similar to those I shall describe below for a later layer (G), except that the cell types found for intermediate parameter values (e.g., the "bilobed" cells to be discussed) are, in layer D, less robust against random variations in initial conditions. The difference between development in layer D vs. that in layer G results from the shallower form of Mexican-hat Q function in the earlier layer.

Choose layer-D parameters that lead to the emergence of substantially circularly symmetric ON-center cells in layer D. Example parameter values are $n_{ED} = 0.5$, $r_D/r_C = 1$, $k_1 = 0.32$, $k_2 = -3$; these choices lead to D cells having $g = 0.12$. These values are intended to aid the reader in reconstructing a representative case. Similar results are obtained for other values, provided r_D is small compared to $s_{min} = 1.74r_C$. The mature g value is essentially constant for all D cells (independent of random initial conditions) and is given approximately by $\bar{k}$.

Extension to Further Layers. Having found that a D layer of ON-center cells emerges (in an appropriate regime of parameter space), we can calculate $Q^D(s)$ by using the same idealization as above and by using the continuum form (above) of Eq. 2. We obtain a Mexican-hat form, with a zero-crossing at $s = 1.23r_D$ and a minimum of -0.20 at $s_{min} = 1.81r_D$.

If the same calculation is repeated for a couple more layers, with $r_F = r_E = r_D$ and with $g = 0.12$ at each stage (our use of the same g values and arborization radii at each of these stages is arbitrary and inessential), the Mexican-hat form becomes more pronounced: its minimum, relative to its peak, deepens to become -0.25 and -0.27, located at $s_{min} = 1.84r_E$ and $1.90r_F$, in layers E and F respectively. The amount of further deepening decreases with additional layers of this type; the Mexican-hat minimum would be -0.346 at the tenth ON-center layer and -0.355 at the fourteenth, if we were to continue this process.

Let us carry this process through layer F. This choice of four layers of ON-center cells is partly arbitrary, yet motivated by the observation that there are about this number of stages in the retinogeniculocortical pathway between the first appearance of opponency (in the retinal bipolar cells) and the first orientation-selective cells in cortex (see *Discussion*).

The "Internal Environment" Seen by a Layer Is Self-Structured by the Network. Suppose a developing layer of our system were directly exposed to an ensemble of striped patterns of sinusoidally varying "illumination" (input activity) having fixed wavenumber k_Q but with each pattern having random stripe orientation and phase. The function $Q(s)$ for this ensemble can be explicitly computed: it is the Bessel function $J_0(k_Q s)$. If we choose $k_Q = 1.92/r_F$, then the locations of the first three zero-crossings and of the Bessel-function minimum, as well as the Bessel-function's values (up to the first zero-crossing), all coincide (to within a few percent) with those of our Q^F function. The Bessel function's minimum is deeper: -0.40 compared with -0.27. (This correspondence is not an accident of parameter choices; it is found using other sets of g values as well.)

The striking point is that our layer G sees an ensemble of presentations whose two-point correlation statistics are qualitatively very similar to those of an ensemble of striped patterns, even though the input activity to layer G starts out as totally random and uncorrelated activity in layer A.

Development of Layer G: Emergence of Orientation-Selective Cells. We shall now explore the parameter regime for G-cell development. Many of the same qualitative features emerge at earlier stages (D through F) for appropriate parameter-value choices. However, we wish to focus on characteristic features that arise from the Mexican-hat form of Q, and those features become more clear when the Mexican-hat form is more pronounced.

By use of the Mexican-hat Q^F derived above, mature morphologies were computed for layer-G cells for $n_{EG} = 0.5$ and for a range of r_G/r_F, k_1, and k_2 values. Below, I summarize the results of over 170 development runs (using Eq. 1) for r_G/r_F ranging from 1 to 4 and $\bar{k}$ ranging from 0 to 0.5, with k_2 negative (typically $k_2 = -3$, but, as noted earlier, results are insensitive to the value of k_2 at given $\bar{k}$). The same morphologic regimes were found in 120 simulated-annealing (9) runs, in which global near minima of Eq. 3 were calculated. Reversing the sign of k_1 (and hence of $\bar{k}$) and changing n_{EG} to $1 - n_{EG}$ changes excitatory regions to inhibitory regions, and vice versa, but otherwise leaves the mature morphology unchanged.

For r_G small compared to s_{min} (e.g., $r_G/r_F = 1$): As the mature g value is decreased by decreasing $\bar{k}$, the cell type changes from all-excitatory ($g = 0.5$), to approximately circularly symmetric ON-center ($0.5 > g \gtrsim 0.1$), to an opponent type having an increasingly eccentric core, to a cell type in which an excitatory and an inhibitory region are separated by an arced or straight boundary passing near the cell's center ($g \simeq 0$). This is the same behavior as was found for layers C (paper 1) and D (above).

For large r_G/r_F (e.g., 4): As the mature g value is decreased, we pass from the all-excitatory regime, to one in which there are isolated inhibitory islands (i.e., regions in which the c values have reached their inhibitory limit) in an excitatory sea, to one in which the inhibitory regions are band-like. For $g \simeq 0$, the total numbers of synapses lying in excitatory and inhibitory regions are equal (when $n_{EG} = 0.5$), and we find alternating bands of excitatory and inhibitory character that are generally locally parallel (Fig. 1) but can have occasional branching and blind endings. The width of each band is of order s_{min} (= $1.90r_F$ for our particular Q^F function).

For r_G of order s_{min} (e.g., 1.7–2.0r_F): The Q^F function reaches its minimum at intersynaptic separations of the order of the F-to-G arborization radius r_G. As the mature g is decreased, we pass from the all-excitatory regime, to one having several inhibitory islands (typically three, hence a "trilobed" cell regime) spaced around the cell's center. For intermediate g (between approximately 0.15 and 0.3, for $r_G/r_F = 1.7$), the number of islands is two ("bilobed" cell regime). These inhibitory lobes are disposed about the cell's center with rough bilateral symmetry (Fig. 2) and with an orientation that varies randomly from cell to cell. The width of the inner excitatory band which traverses the cell is of order s_{min}. The edges of this band are approximately straight and parallel (more so when the lobes are at nearly equal distances from the cell's center). As g is decreased further, the inhibitory lobes join peripherally to form a "C" shape or to enclose completely an ovoid excitatory core; this inhibitory surround is in turn enclosed by an outermost excitatory ring. For $g \simeq 0$, the core shifts away from the cell's center, and a set of alternating band-like regions whose shape varies from cell to cell (e.g., they may be straight or "C"-shaped) develops.

At constant $g = 0.20$, as we increase r_G/r_F, we pass from a circularly symmetric ON-center cell, to an "ovoid-core" cell (at $r_G/r_F \simeq 1.4$), to a "bilobed" cell ($r_G/r_F \simeq 1.6$–2.1), to a "trilobed" cell, and finally to a cell having many inhibitory islands in an excitatory sea.

Thus the bilobed cell regime occupies a "bubble" in the (r_G/r_F, g_{mature}) parameter space. At the boundaries between

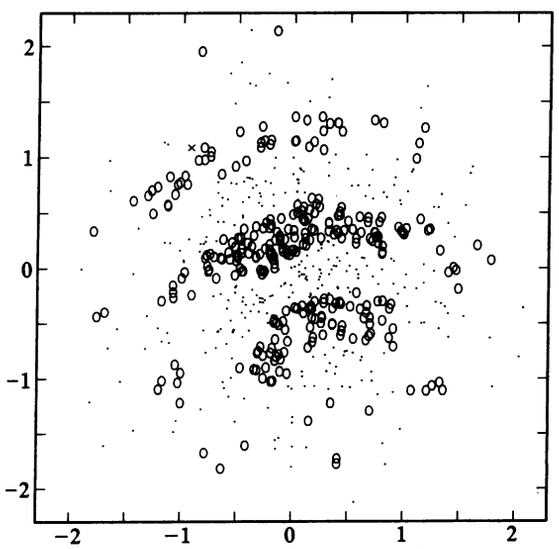

FIG. 1. Synaptic positions and connection strengths at maturity for a single cell of layer G having 600 synapses, placed randomly according to a two-dimensional Gaussian distribution. Parameter values are $n_{EG} = 0.5$, $r_G/r_F = 4$, $k_1 = 0$, $k_2 = -3$. Connection strengths are indicated as ovals, for $c = -0.5$, and dots, for $c = +0.5$; x represents intermediate c (one point only). Axis values are in units of r_G.

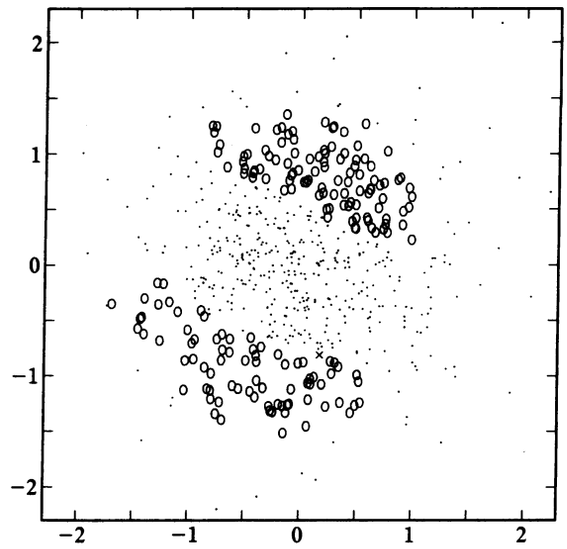

FIG. 2. A bilobed G cell. Parameter values are $n_{EG} = 0.5$, $r_G/r_F = 1.8$, $k_1 = 0.6$, $k_2 = -3$. Symbols are as in Fig. 1.

regimes, cell-to-cell variations in random initial conditions lead to more than one morphology being represented (i.e., a morphologically nonuniform layer). Well within a regime, substantially all cells of the G layer develop the same mature morphology. For example, at $r_G/r_F = 1.8$, $k_1 = 0.6$, $k_2 = -3$, eight runs (including that of Fig. 2) yielded eight bilobed cells having $g = 0.194$–0.197, each with an inner excitatory band whose width is $(2.1 \pm 0.1)r_F$ (defined by fitting each band by a bar of some width and calculating the mean and standard deviation of these bar widths) and whose center line is displaced from the cell's center by $(0.2 \pm 0.2)r_F$.

Response to an Experimental Test Stimulus. Illuminate layer A with a test stimulus consisting of stripes of light and dark illumination (say $F^A = 1$ or 0 for each stripe), each stripe having width w. Calculate the resulting activity in mature layers B–F. The response of the G cell of Fig. 2 depends upon the orientation and position of the stripes relative to the cell. Calculate the difference between maximal and minimal response of that G cell as the striped pattern is passed over it, as a function of the stripe orientation relative to the G-cell's axis. This gives the orientation tuning curve for the G cell. Let $w \simeq 2.15r_F$, the width of the central excitatory band. Then the value of this tuning function is maximal on-axis, has a minimum (whose value is 8% of the maximum) at ≃90° off-axis, and has a "half-width at half-maximum" of 38°.

DISCUSSION

I have shown the following. (*i*) One or more layers (in series) of opponent cells produce an activity autocorrelation function Q that is of "Mexican-hat" form. An idealization that facilitates the development calculations has been introduced and discussed. (*ii*) The more such layers, the more pronounced is the Mexican-hat character of Q. (*iii*) Orientation-selective cells whose transfer function (spatial arrangement of c values) is of banded excitatory/inhibitory character, as in Figs. 1 and 2, appear to be among a fairly small range of possible solutions in a layer whose development is governed by a Mexican-hat type of Q function.

Why Does a Mexican-Hat Q Function Produce Banded and Bilobed Cells? (*i*) First suppose synaptic density were uniform (rather than Gaussian) and that $k_1 = k_2 = 0$. The minimization of the E_n function of Eq. 3, for a Mexican-hat Q^L, favors each point being like its near-neighbors (in its excitatory or inhibitory character) and unlike its midrange-neighbors. But

each point cannot be the center of a "like" island in an "unlike" sea. The mature solutions of Eq. 1—or, equivalently, the Hebb-optimal states of Eq. 3—correspond to a "compromise" that consists of parallel stripes of excitatory and inhibitory character, the orientation of the stripes being arbitrary. The stripe boundaries are straight in order to minimize the interaction energy between pairs of unlike near-neighbors. (*ii*) Since the synaptic density is greater centrally, E_n minimization can favor minimizing the core's interaction energy at the expense of the periphery. This leads to a spectrum of solutions having various degrees of circularly symmetric vs. striped character, as we have found.

Biological Relevance. In the visual system, we can loosely identify layer A of our system with the photoreceptor cell layer; layer B with the intraretinal convergence of inputs; opponent-cell layers C–F with bipolar and retinal ganglion cells, and possibly (see below) cells of lateral geniculate and of layer IVc of primary cortex; and layer G with the orientation-specific "simple" cells of layer IVb and other layers of primary cortex.

In fact, our bilobed G-cell type, and the type having an excitatory and inhibitory region separated by a straight line passing through the cell's center, match Hubel and Wiesel's qualitative depiction (figure 2 of ref. 2) of the receptive fields of "simple" cells in cat. (I explicitly find that the response of our G cell of Fig. 2 to point-source illumination in layer A has a central band-like excitatory region with inhibitory bilobes.)

I say "loosely identify" since I have not attempted here to model the retina (1). Also not treated is the case in which a physical layer is shared by two or more different cell populations, with each population developing according to its own set of parameters and possibly receiving inputs from different source layers. These complications can be analyzed within the modular self-adaptive network framework. Their analysis may prove relevant to understanding the organization of color-processing and other subsystems.

If our network fairly represents what happens during the development of the first few stages of a biological visual system, we may obtain several insights (or at least useful hints) from its behavior thus far.

(*i*) It was noted that bilobed-cell formation is morphologically more uniform in layer G than it is in layer D, for parameter values lying in the appropriate regime in each case. The difference is that the series of opponent-cell layers C–F deepens the minimum of the Mexican-hat Q^F function compared with Q^C. Opponent-type *receptive fields* have been measured for retinal ganglion cells and cells of lateral geniculate and cortex. It is not clear from these experiments whether the *transfer functions* (from one layer to the next) are of opponent type. If they are, my analysis suggests a role that this multiplicity of opponent-cell layers may serve: it may generate the ensemble statistical properties needed to facilitate the emergence of a uniform layer of well-tuned orientation-selective cells (e.g., of bilobed type) in cortex.

(*ii*) Signal-to-noise considerations (1) led to approximate inequalities relating the number of synapses per neuron, cell body size, arborization breadth, and layer maturation time in our system. This type of analysis may help us to understand better the relationships, in biological systems, between neuronal "device properties" and a network's capacity for self-adaptive development of feature-analyzing cell layers.

(*iii*) None of the assumptions I have made is specific to visual processing, and I have focused on the case in which there is no environmental input to the network. This suggests that the same relatively limited set of morphologic options may be common to the early stages of visual and other perceptual subsystems.

(*iv*) My approach ascribes complementary roles to three factors that can influence the development of neural architectures. First, development-rule-induced constraints determine the range of morphologic options for each layer in turn. Second, the particular choices of parameter values may reflect particular statistical features or constraints of the visual (or other perceptual) environment in a biological system subject to evolutionary adaptive pressures. These pressures might, for example, select for the formation of contrast-selective or orientation-selective cell layers, from among the available morphologic options. Third, the individual's perceptual experience affects the statistics of the input ensemble (e.g., the Q^A function) that "trains" the system, when such experience is available during the maturation process (a case not treated here). The fuller understanding of how these complementary factors mold neural development is an exciting challenge for future work, both experimental and theoretical.

1. Linsker, R. (1986) *Proc. Natl. Acad. Sci. USA* **83**, 7508–7512.
2. Hubel, D. H. & Wiesel, T. N. (1962) *J. Physiol.* **160**, 106–154.
3. Hubel, D. H. & Wiesel, T. N. (1977) *Proc. R. Soc. London Ser. B* **198**, 1–59.
4. Wiesel, T. N. & Hubel, D. H. (1974) *J. Comp. Neurol.* **158**, 307–318.
5. Fregnac, Y. & Imbert, M. (1984) *Physiol. Rev.* **64**, 325–434.
6. Von der Malsburg, C. & Cowan, J. D. (1982) *Biol. Cybern.* **45**, 49–56.
7. Bienenstock, E. L., Cooper, L. N. & Munro, P. W. (1982) *J. Neurosci.* **2**, 32–48.
8. Braitenberg, V. (1985) in *Cerebral Cortex*, eds. Jones, E. G. & Peters, A. (Plenum, New York), Vol. 3, pp. 379–414.
9. Kirkpatrick, S., Gelatt, C. D. & Vecchi, M. P. (1983) *Science* **220**, 671–680.